A&A 439, 1171–1181 (2005)
DOI: 10.1051/0004-6361:20052821
© ESO 2005

Astronomy & Astrophysics

Kinetic vs. multi-fluid models of H atoms in the heliospheric interface: a comparison

D. Alexashov[1,3] and V. Izmodenov[2,3,1]

[1] Institute for Problems in Mechanics, Russian Academy of Sciences, Prospect Vernadskogo 101-1, Moscow 119526, Russia
[2] Lomonosov Moscow State University, Department of Mechanics and Mathematics & Institute of Mechanics, Moscow 119899, Russia
[3] Space Research Institute (IKI) Russian Academy of Sciences, Moscow, Russia
e-mail: izmod@ipmnet.ru

Received 4 February 2005 / Accepted 18 April 2005

Abstract. The goal of this paper is to illuminate similarities and differences in the kinetic and multi-fluid models of the heliospheric interface, the region of solar wind interaction with the Local Interstellar Cloud (LIC), and then to explore physical reasons for these differences. We present a detailed comparison of two types of models. The first type is based on a kinetic description of the interstellar H atom flow, which is required for this problem due to the fact that the mean free path of H atoms is comparable to the characteristic size of the heliospheric interface. The second type of model is based on a voluntary assumption that the flow of H atoms can be described hydrodynamically by a set of Euler equations (one-fluid approach) or by 2, 3, and 4 sets of Euler equations for different populations of H atoms (thus 2-, 3-, or 4- fluid models). It is shown that differences are significant between kinetic and multi-fluid models in observationally meaningful measurements such as the location of the termination shock and heliopause, the filtration of H atoms through the heliospheric interface, and the velocities and temperatures of H atoms. Therefore, the multi-fluid models may lead to incorrect interpretation of observational data.

Key words. Sun: solar wind – interplanetary medium – ISM: atoms

1. Introduction

Interstellar atoms of hydrogen are of major importance for heliospheric interface studies because: 1) H atoms form the most abundant component in the circumsolar interstellar medium; 2) major observational information on the heliospheric interface is connected with the interstellar atoms. Interstellar H atoms are coupled to both the interstellar plasma and the solar wind by charge exchange. Therefore, it is important to take the interstellar neutral component into account self-consistently with the plasma component in the models.

The qualitative pattern of the heliospheric interface is shown in Fig. 1. The supersonic solar wind plasma decelerates at the termination shock (TS) to subsonic, while the interstellar plasma decelerates at the bow shock (BS). The heliopause (HP), which is a contact discontinuity, separates these two plasma flows. In contrast to the plasma component, which deviates at the heliopause, interstellar hydrogen atoms (H atoms) penetrate deep into the heliosphere. Inside the heliosphere at one or several AU the H atoms and their derivatives, such as pickup ions and anomalous cosmic rays (ACRs), can be measured. The momentum transfer cross sections of elastic H-H, H-p collisions are negligible as compared with the charge exchange cross section (Izmodenov et al. 2000). The charge exchange process strongly influences the properties of the H atom gas in the interface. Hydrogen atoms newly created by charge exchange have the velocities of their ion partners in the charge exchange collisions. Therefore, the parameters of these new atoms depend on local plasma properties. It is convenient to distinguish four different populations of H atoms: 1) atoms created in the supersonic solar wind (so-called neutral solar wind); 2) atoms originating in the inner heliosheath and known as heliospheric ENAs (e.g., Gruntman et al. 2001; Izmodenov et al. 2001b; McComas et al. 2004); 3) atoms created in the disturbed interstellar wind; 4) original (or primary) interstellar atoms. The strength of H atom-proton coupling can be estimated by calculating mean free path of H atoms in plasma. It could be shown (e.g., Izmodenov 2000) that the mean free paths of the H atom populations with respect to charge exchange with protons are comparable to or larger than the size of the heliospheric interface. Therefore, the kinetic Boltzmann approach must be used to describe interstellar atoms in the heliospheric interface correctly.

The first self-consistent model of the heliospheric interface has been suggested by Baranov et al. (1991) and developed by Baranov & Malama (1993). Interstellar H atoms were described in the model kinetically, while the charged component was considered as an ideal fluid. Results of this

Article published by EDP Sciences and available at http://www.edpsciences.org/aa or http://dx.doi.org/10.1051/0004-6361:20052821

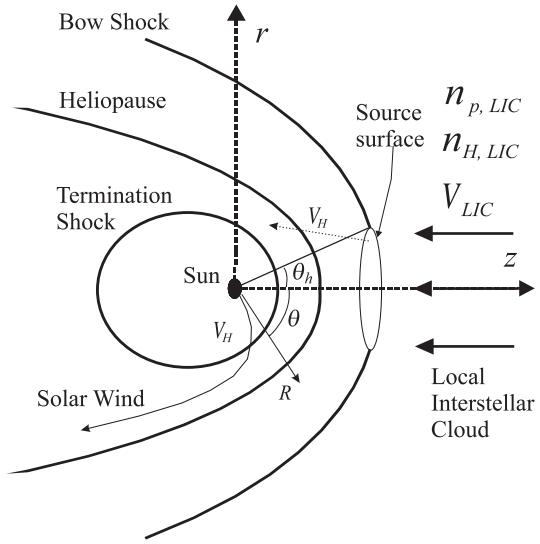

Fig. 1. The qualitative pattern of the heliospheric interface – the region of the solar wind interaction with LIC. A "source surface" at the bow shock in the upwind direction for specific test calculations described in Sect. 3.6. The size of the "source surface" depends on angle θ_h. Cylindrical and spherical system of coordinated are shown, respectively, as (r, Z) and (R, θ).

Baranov-Malama model were also discussed in Baranov & Malama (1995, 1996), Izmodenov et al. (1999), and Izmodenov (2000). Later this kinetic-continuum model has been advanced by taking into account additional physical effects, such as solar cycle variations of the solar wind (Izmodenov & Malama 2004a,b; Izmodenov et al. 2005), influence of the interstellar magnetic field (Alexashov et al. 2000), interstellar ionized helium and solar wind alpha particles (Izmodenov et al. 2003b), galactic cosmic rays (Myasnikov et al. 2000), and anomalous cosmic rays (Alexashov et al. 2004b). For recent reviews of developments by the Moscow group see Izmodenov (2003, 2004). A kinetic description of the interstellar atoms was also used in the models by Lipatov et al. (1998) and Müller et al. (2000). Differences between the Baranov-Malama and Lipatov-Zank-Müller models are discussed later in this paper.

Even through the interstellar H-atoms were described kinetically in the first self-consistent Baranov-Malama model, one-fluid and multi-fluid descriptions of the interstellar H atom component in the heliospheric interface were extensively employed in quite large number of publications (Zank et al. 1996; Pauls & Zank 1997; McNutt et al. 1998, 1999; Wang & Belcher 1998, 1999; Fahr 2000; Fahr et al. 2000; Fahr & Scherer 2003a,b; McNutt 2003, 2004; Florinski et al. 2003, 2004, and others). The one-fluid approach assumes that the velocity distribution function of H atoms is Maxwellian. This assumption is actually equivalent to the assumption of effective elastic H-H collisions, of weak H-p elastic collisions and a weak charge exchange. In other words, it is assumed in the one-fluid model that the mean free path of H atoms, calculated with respect to H-H collisions, is much smaller than both the characteristic size of the problem and the mean free path, calculated with respect to charge exchange. In the multi-fluid approaches all H-atoms are divided into several populations dependening on the model, then it is assumed that each population can be described by Euler's equations for ideal fluids. The total velocity distribution function of H atoms is assumed to be the sum of the Maxwellian velocity distributions of different populations.

It is very natural to divide interstellar H atoms into four populations that depend on four regions of the heliospheric interface as described above. However, to our knowledge such four-fluid H atom models have not yet been employed. Instead, models with three H atom fluids (after Zank et al. 1996) and models with one-H-atom fluid (e.g. Fahr et al. 2000) appear in the literature. For the purposes of comparison in this paper we consider four different multi-fluid H-atom models, including the four-fluid H atom model.

It is worth noting that the velocity distribution functions of the four introduced populations of H-atoms were calculated explicitly by Izmodenov (2001) and Izmodenov et al. (2001a). It was clearly concluded in the papers that neither the velocity distribution function, in total, nor the velocity distributions of separate populations are Maxwellian. This means that one-fluid or multi-fluid approach approximations are not valid for the solar wind/LIC interaction problem. Results of one of the most sophisticated – with the respect to H-atom populations – of the existing multi-fluid models (Zank et al. 1996) were compared to the results of the kinetic Baranov-Malama model by Baranov et al. (1998). This comparison shows essential qualitative and quantitative disagreements in distributions of H atoms. McNutt (2004) compared one-fluid and kinetic models for different values of interstellar electron number densities and found significant differences in the hydrogen wall and the filtration of H atoms.

Despite the fact that the basic assumption of the fluid approximation requiring the mean free path to be much smaller than the characteristic size of the problem, is not fulfilled for the H atoms in the heliosphere, interest in multi-fluid models does not decreased (e.g., Zank & Müller 2003; Scherer & Fahr 2003a,b; McNutt 2003, 2004). This is connected with the fact that numerical methods solving gas dynamic or MHD equations are much more developed and with the possibility of adopting the existing gas dynamic or MHD codes to modeling the heliospheric interface. In contrast, to solve the kinetic equation for H atoms is not all that easy; one way to solve it in the interface is to use the Monte Carlo method. However, the so-called direct simulation Monte Carlo (DSMC) method is not effective, because of the fairly complex geometry of the problem. Instead one should develop Monte Carlo methods with splitting of trajectories as developed by Malama (1991). Splitting trajectories improves the efficiency of Monte Carlo code by $\sim 10^5 - 10^6$ times (Malama 1991). Note that the particle mesh method developed by Lipatov et al. (1998) is somewhat equivalent to DSMC methods. As an alternative to Monte Carlo methods the kinetic equation for H atoms has been solved directly by Osterbart & Fahr (1992).

In this paper we come back to comparison of the kinetic and multi-fluid models of the heliospheric interface. There are two reasons for this. First, we want to explore differences in the models for values that can be determined from available spacecraft data: 1) distances to the termination shock and the heliopause; 2) the number density, velocity, and temperature of

the interstellar H atoms at the heliospheric termination shock. The distance to the termination shock provides very important constraints to models of the heliospheric interface, because the Voyager 1 spacecraft is apparently in the vicinity of the TS and apparently has crossed or will cross the TS in the very near future (Krimigis et al. 2003; McDonald et al. 2003). The number density of interstellar H atoms at the termination shock can be estimated from analysing pickup spectra measured by Ulysses/SWICS and ACE/SWICS (Gloeckler & Geiss 2004). The density can be deduced from deceleration of the supersonic wind measured on Voyagers (Richardson 1997; Wang & Richardson 2003; Richardson et al. 2004). In addition, the density, velocity, and temperature of H atoms at the TS can be derived from a large number of H cell Lyman alpha data obtained by SOHO/SWAN (e.g. Lallement et al. 2005, and references therein).

The second goal of this paper is to clarify the physics of the difference between kinetic and multi-fluid models. This might possibly lead to future improvements in the simplified multi-fluid models to make them more appropriate for dealing with some aspects of heliospheric interface modelling.

2. Models

For the purposes of comparison in this work we restrict ourselves to as simple an axisymmetric model of the heliospheric interface as possible. We assume that the local interstellar medium consists of two-components: an ionized component (electrons and protons) and a neutral one (H atoms). These two components interact by charge exchange only. Photoionization and electron impact ionization are neglected in this paper for the sake of simplicity. All charged particles (electrons, protons, pickup ions) are considered as a single fluid with total density ρ and bulk velocity $\boldsymbol{V}$. It is assumed that all ionized components have the same temperature T. Although this assumption cannot be made in the case of the solar wind, the one-fluid solar wind model is based on mass, momentum, and energy conservation laws, and it predicts the plasma bulk velocity and locations of the shocks very well (Malama et al. 2005, in preparation). Magnetic field and both anomalous and galactic cosmic rays are ignored in the paper.

To describe the charged component we solve fluid Euler equations with the sources of momentum and energy in the right parts of these equations. The sources of momentum and energy in the Euler equations will be specified for the kinetic and multi-fluid models separately. The temperature of the plasma is determined from the equation of state, $p = 2n_{\rm p}kT$, where k is Boltzman's constant, $n_{\rm p}$ – the proton number density, and γ is assumed to be 5/3.

Boundary conditions for the charged component are determined by the solar wind parameters at the Earth's orbit and by parameters in the undisturbed LIC. At the Earth's orbit it is assumed $n_{\rm p,E} = n_{\rm e,E} = 7$ cm^{-3}, $V_{\rm E} = 375$ km s^{-1}, $T_{\rm E} = 51\,109$ K. For the pristine interstellar medium we adopt: $V_{\rm LIC} = 26.4$ km s^{-1} and $T_{\rm LIC} = 6527$ K (Möbius et al. 2004; Witte 2004; Gloeckler et al. 2004; Lallement 2004a,b), $n_{\rm H,LIC} = 0.18$ cm^{-3}, $n_{\rm p,LIC} = 0.06$ cm^{-3} (for argumentation see, e.g., Izmodenov et al. 2003, 2004). The outflow boundary conditions in the tail region are assumed to be soft boundary conditions. For details of the computations in the tail direction see Izmodenov & Alexashov (2003), Alexashov et al. (2004a).

2.1. Kinetic model for the heliospheric H-atoms

In the continuum-kinetic model (Baranov-Malama model), hydrodynamic equations for the charged component are solved self-consistently with the kinetic equation for the velocity distribution function of H atom component, $f_{\rm H}(\boldsymbol{r}, \boldsymbol{w}_{\rm H}, t)$ (e.g., Izmodenov 2004). We assume in this paper that the solar gravity force is in balance with the solar radiation pressure force. The right parts of the Euler equations for the charged component are expressed through integrals of $f_{\rm H}(\boldsymbol{r}, \boldsymbol{w}_{\rm H}, t)$. The explicit expressions for these integrals are given in Izmodenov (2004).

The boundary condition for the kinetic equation is given in the pristine LIC. It is assumed that the H atom flow has the same velocity and temperature as the plasma flow, and for H atom number density it is assumed that $n_{\rm H,LIC} = 0.18$ cm^{-3} (Izmodenov et al. 2003, 2004). The velocity distribution function is assumed to be Maxwellian in the LIC.

2.2. Multi-fluid models

In this section we describe multi-fluid approaches for the interstellar H atom flow in the heliospheric interface. Governing equations and boundary conditions for the plasma component are as previously described.

It is supposed in multi-fluid models that H-atoms in the heliospheric interface can be divided into N populations, and the velocity distribution functions of these populations are locally Maxwellian with parameters ρ_i, $\boldsymbol{V}_i$ and T_i, where $i = \overline{1, N}$. Since H atoms newly created by charge exchange have properties of the local protons, it is very convenient to divide H atoms into several populations depending on the place of their origin. Therefore, atoms of population i originate in region i of the heliospheric interface. Note, that for a one-fluid model of H atoms $N = 1$, and all H atoms in the heliospheric interface are considered as one fluid. Different populations of H atoms do not interact each with other, but they interact with the plasma component by charge exchange. Governing equations for i-component of H atoms have the same form as those for the plasma component with the source terms in the right parts, q_{i1}, $\boldsymbol{q}_{i2}$, and q_{i3} that describe interaction by charge exchange of population i of H-atoms with the proton component. The equation of state for each neutral component is $p_i = n_i k T_i$, which is different from the state equation of the charged component. In this paper we use the expressions of the source terms given by McNutt et al. (1998). Although we do not present results in the paper, we performed test calculations with the source terms given by Zank et al. (1996). These source terms provide results, which are very close to that given by McNutt et al. (1998). The sources in the plasma Euler equations are equal to the sum of the sources of all fluids of H atoms with opposite sign.

For the purpose of comparison with our kinetic model we developed four different multi-fluid models (models $F1$, $F2$, $F3$, and $F4$). In model $F1$ we do not divide H-atoms into

sub-populations and consider all H-atoms as a single fluid. This model corresponds to the description of H-atoms by Fahr et al. (2000). It is important to note here that to get a steady solution in the one-fluid model we neglected the H atoms originating in the supersonic solar wind, although massloading of the solar wind plasma was taken into account properly, a similar procedure was followed by Fahr et al. (2000). Note that here, unlike in other papers, N-fluid model means N-fluid approach used for H atoms flow.

In the model $F2$ H-atoms are separated into two populations: 1) atoms originated (by charge exchange) in the heliosphere inside the heliopause; 2) atoms originating in the interstellar medium outside the heliopause including primary interstellar H atoms. As described in the previous section, each of the two populations is assumed to have a Maxwellian distribution function.

In model $F3$ we divide atoms created inside the heliopause into two populations: 1) atoms created in the supersonic solar wind region inside the TS; 2) atoms created in the inner heliosheath, the region between the TS and HP. Therefore, it is assumed in this model that the velocity distribution of H atoms in the heliospheric interface is a sum of three Maxwellian. This model corresponds to the description of H atoms chosen in Zank & Pauls (1996), Müller (2000), Florinski et al. (2004), etc.

Finally, in $F4$ model H atoms in the heliospheric interface are divided into four populations: 1) atoms created in the supersonic solar wind region inside the TS; 2) atoms created in the inner heliosheath, the region between the TS and HP; 3) atoms created in the outer heliosheath between the HP and BS; and 4) primary interstellar H atoms entering the interface from pristine interstellar medium.

Outer inflow boundary conditions for the total H atom flow in $F1$ model, both for the interstellar atoms population in $F2$ and $F3$ models and for the primary interstellar H atoms of $F4$ model, coincide with the boundary conditions of the kinetic model: $V_{\rm LIC} = 26.4$ km s^{-1}, $T_{\rm LIC} = 6527$ K, and $n_{\rm H,LIC} = 0.18$ cm^{-3}. For outflow boundaries, which are 1) the outer boundary in the tail direction for all populations; 2) inner boundary at 1 AU; 3) outer boundary in all directions for population 1 of $F2$-model, populations 1 and 2 of $F3$-model and population 1, 2, and 3 of $F4$-model, we adopt soft boundary conditions. We applied first and second order extrapolation procedures at these boundaries and apparently the boundary conditions do not change model results.

2.3. Method for solving the system of governing equations

To solve the system of governing Euler equations for the plasma component, the second order finite volume Godunov-type numerical method was used (Godunov et al. 1979; Hirsch 1988). To increase the resolution properties of the Godunov scheme, a piecewise-linear distribution of the parameters inside each cell of the grid is introduced. To achieve the TVD property of the scheme the *minmod* slope limiter function is employed (Hirsch 1988). We used adaptive grid as in Malama (1991), which fits the termination shock, the heliopause and the bow shock. To fit the discontinuities, the soft-fitting technique developed by Myasnikov et al. (1997) is adopted. In the continuum-kinetic model (Baranov-Malama model) we solve the kinetic equation by Monte-Carlo method with splitting of trajectories as developed by Malama (1991). To get a self-consistent solution of the plasma Euler equations and kinetic equation we used the method of global iterations suggested by Baranov et al. (1991).

In the case of multi-fluid models, we applied the same Godunov type of numerical method for all populations of H-atoms. All systems of Euler equations were solved simultaneously and computational grids coincide for the plasma component and for all components of H-atoms. Here we should note that there is fundamental difference between flows of plasma and H-atoms. In the case of plasma, the solar wind flow and flow of charged components of the interstellar medium meet at a contact discontinuity – the heliopause, which separates two flows. Then, the heliopause can be considered as an obstacle for both the solar wind and interstellar plasmas. Since both flows are supersonic, two shocks should appear in the solar wind and the interstellar medium. In the case of pure gasdynamics (no H atoms) this picture of two shocks and contact discontinuity could be constructed prior to any computations. Influence of the charge exchange could change the plasma flow pattern, but this does not happen for chosen realistic interstellar parameters. For fluids of H-atoms the situation is different since: 1) a priori there is no boundary (as the heliopause for the plasma component), which can serve as an obstacle for the fluid of H-atoms; 2) there are sinks and sources into the governing equations, which often determined the flow of H atoms (see, e.g., Izmodenov et al. 2005). Therefore, for numerical calculations we cannot construct the qualitative picture of H-atom population flows. It means that we can neither recognize nor fit any potential discontinuities in the H atom flow as we do for the plasma component. At the same time our numerical method can capture the shocks or other discontinuities that may appear in the flow of H atoms.

3. Results

To make a detail comparison between the kinetic and multi-fluid approaches we performed a number of model calculations and numerical tests.

3.1. Comparison of self-consistent kinetic and multi-fluid models

First, we compare the self-consistent kinetic (Baranov-Malama) model of the heliospheric interface (set "K") to four self-consistent multi-fluids models $F1$–$F4$, which were described in Sect. 2. Figure 2 shows the shapes and locations of the termination shock, heliopause, and the bow shock for the five self-consistent models discussed above. The termination shock and heliopause are located farther from the Sun in the case of the multi-fluid H-atom models compared to the kinetic model. The more fluids in the model, the closer the position of the TS to the kinetic solution (Table 1). The results

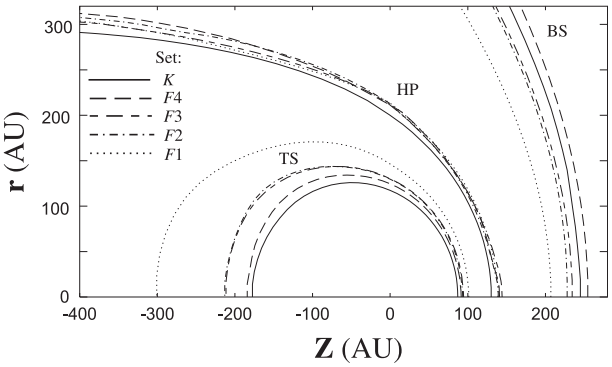

Fig. 2. The termination shock, heliopause and bow shock for the self-consistent models K and $F1$–$F4$. The models details are given in Sect. 2. TS, HP and BS are designations of termination shock, heliopause and bow shock, respectively. The solid (K), dashed ($F4$), long-short dashed ($F3$), dashed-dotted ($F2$) and dotted ($F1$) curves correspond to kinetic, four-fluid, three-fluid, two-fluid and one-fluid H-atom models, respectively. Z is the heliocentric distance (in AU). Axis OZ is directed towards the interstellar gas flow.

Table 1. Distances to the termination shock, heliopause, and bow shock in the upwind direction in AU (%).

Set	Termination shock	Heliopause	Bow shock
K	87 (100%)	130 (100%)	245 (100%)
$F1$	101 (+16%)	139 (+6.8%)	207 (–15%)
$F2$	93 (+7.9%)	139 (+6.9%)	228 (–7%)
$F3$	94 (+8%)	144 (+10.8%)	234 (–4.5%)
$F4$	91 (+4.6%)	141 (+8.5%)	254 (+3.7%)

that are closest to the K-model are provided by the $F4$ model, which gives 5% less difference for the distance to the termination shock. The heliocentric distance to the heliopause is nearly the same for all multi-fluid models. The differences between all the multi-fluid models in the location of the HP are 1−3 AU (Fig. 2), whereas the differences between the multi-fluid and kinetic models consist of ∼10 AU. The difference with the kinetic model in the distance to the bow shock may reach up to ∼40 AU for $F1$-model, while the $F4$-model gives the closest result as compared with the kinetic model (Table 1).

Figure 3 presents number densities, velocities, and temperatures for plasma and H-atom components in the upwind direction for the five self-consistent models ($K, F1, F2, F3, F4$). In the kinetic model we compute the number density, velocity, and temperature of H-atoms as corresponding integrals of the velocity distribution function. In the multi-fluid models ($F2, F3, F4$) the number densities of H atoms are calculated as the sum of number densities of all populations. As for their velocity and temperature we adopt weighted averages for all populations of H-atoms.

Qualitatively, the distributions of plasma parameters are similar for all models. The results obtained in the frame of the one fluid model, $F1$, provide the largest difference with the results of the kinetic model. The differences in the plasma distributions obtained in all multi-fluid models, $F1$–$F4$,

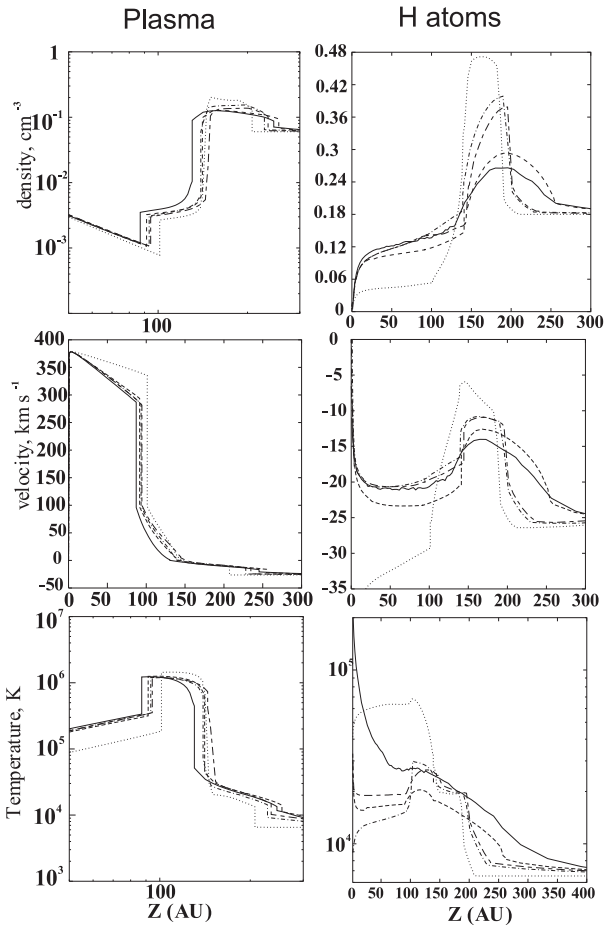

Fig. 3. The number densities, bulk velocities, and temperatures of plasma (*left*) and H atom (*right*) components in the upwind direction for the self-consistent kinetic (K) and multi-fluid models, $F1$–$F4$. The total number density of H atoms represents the sum of number densities of all populations. In the case of multi-fluid models, the bulk velocity and temperature were calculated as weighted averages of the bulk velocities and temperatures of all components. The solid (set K), dashed (set $F4$), long-short dashed (set $F3$), dashed-dotted (set $F2$), and dotted (set $F1$) curves correspond to kinetic, 4-fluid, 3-fluid, 2-fluid and 1-fluid models, respectively.

as compared to the results of the kinetic model, K, are basically connected to the difference in the positions of the heliopause and the shocks. The differences in mass-loading and deceleration of the supersonic solar wind presented in Fig. 3 are connected to different values of the filtration factor (e.g. Izmodenov et al. 2004) of H-atoms through the heliospheric interface, i.e. with different number densities of the H atoms, which penetrate the supersonic solar wind region. Again, the most pronounced difference with the results of the kinetic model is seen for the $F1$-model results.

Differences between the kinetic and multi-fluid models are more pronounced in the distributions of density, velocity, and temperature of H-atoms (Fig. 3, right column). For example, the number density of H atoms in the "hydrogen wall" region (i.e. the region of higher value of the number density of H atoms between the HP and BS as compared to interstellar value) for models $F2$ and $F3$ is two times larger than for the

Table 2. Density, bulk velocity, and temperature of different populations of H atom in the outer heliosphere at 80 AU in upwind.

		Number density,	cm^{-3}	
	1	2	3	4
K	0.26×10^{-3}	0.91×10^{-3}	0.058	0.076
$F4$	0.27×10^{-3}	0.62×10^{-3}	0.054	0.059
$F3$	0.30×10^{-3}	0.41×10^{-3}	0.14	–
$F2$	0.29×10^{-3}	0.14	–	–
$F1$	0.053	–	–	–
		Velocity,	$km\,s^{-1}$	
	1	2	3	4
K	+328.	–5.8	–15.0	–26.9
$F4$	+335.	–16.2	–20.0	–28.0
$F3$	+328.	–54.	–20.5	–
$F2$	+330.	–20.4	–	–
$F1$	–29.	–	–8	–
		Temperature,	K	
	1	2	3	4
K	182 500	67 335	15 490	7100
$F4$	162 200	978 590	16 000	6760
$F3$	195 100	1 218 440	15 630	–
$F2$	194 100	14 870	–	–
$F1$	64 198	–	–	–

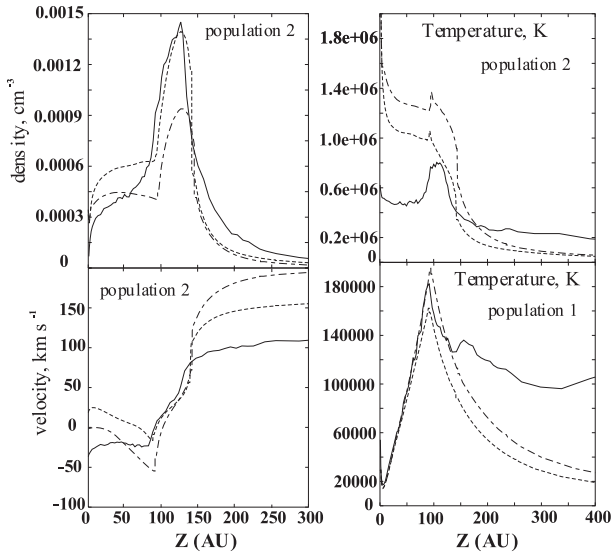

Fig. 4. The density, bulk velocity, and temperature of populations 2 and temperature of population 1 atoms in the upwind direction. The solid (set K), dashed (set $F4$), and long-short dashed (set $F3$) curves correspond to kinetic, 4-fluid, and 3-fluid self-consistent models respectively.

kinetic model. Instead, the hydrogen wall is broader in the kinetic model. Again, $F1$ and $F4$-models give the worst and the best agreement with the K-model, respectively. It is important that the difference between the results of $F4$ and K models is not negligible and could lead to incorrect interpretation of observational data. Table 2 shows the number densities, velocities, and temperatures of H-atoms for different populations in the upwind direction at 80 AU, which is inside the interface for all models.

It is important to note significant differences in the results of the $F3$ and $F4$ models. They are directly connected to the splitting of the interstellar H-atoms (atoms created outside of the heliopause including primary interstellar in $F3$-model) into two populations (primary and secondary H atoms) in the $F4$-model. Indeed, in the region upstream of the bow shock, the bulk velocities of population 4 (original interstellar population) and population 3 (H atoms created in the region between the BS and HP) have opposite directions (e.g., Fig. 5B). Hence, the $F3$-model considers two counterflow populations of H atoms as a one-Maxwellian population. This leads to the large differences in results of these two models. For the same reasons, the H atoms, which originate in the supersonic solar wind (population 1) should be considered separately from the H atoms created in the inner heliosheath, the region between the termination shock and heliopause (population 2). The H atoms of population 2 originate from *hot* postshocked protons and pickup ions. As a result, a significant part of the atoms of this population has large velocities and, therefore, energies. A part of the H atoms of population 2 penetrate back toward the Sun and can be measured at the Earth's orbit as Energetic Neutral Atoms (ENAs). Currently, NASA has plans to launch Interstellar Boundary Explorer (IBEX), a spacecraft which will study the heliospheric interface remotely through measurements of fluxes of the heliospheric ENAs, i.e. fluxes of population 2 (McComas et al. 2004). The number density, velocity, and temperature of population 2 are shown in Fig. 4 for the $F3$, $F4$ and K-models. At the Earth's orbit, these values as obtained by both $F3$ and $F4$-models, (and, therefore, fluxes of ENAs) are drastically different from those obtained in the kinetic model. Interestingly, in the inner heliosheath, the density and velocity of population 2 of the four-fluid model are very close to those of the kinetic model. Apart from the inner heliosheath, the properties of H atoms of population 2 are even qualitatively different, as one can see for the bulk velocity of this population.

Figure 4 also presents radial temperature profile of population 1 of H atoms for the models K, $F3$, and $F4$. In the region outside the termination shock the temperature obtained by three-fluid and four-fluid models decreases with heliocentric distance approximately as $R^{-4/3}$, as it should be in the case of a supersonic point source. Note that Zank et al. (1996) have obtained similar results. At large heliocentric distances beyond the heliopause, the temperature of population 1 of the kinetic model exceeds the temperature of $F3$ and $F4$ models by a factor of 5 or more. This effect clearly shows the kinetic behavior of population 1 of H atoms as compared with fluid models. Note, in addition, that the higher kinetic temperature of population 1 in the kinetic model leads to larger disturbance of interstellar medium in the kinetic model as compared with the multi-fluid models.

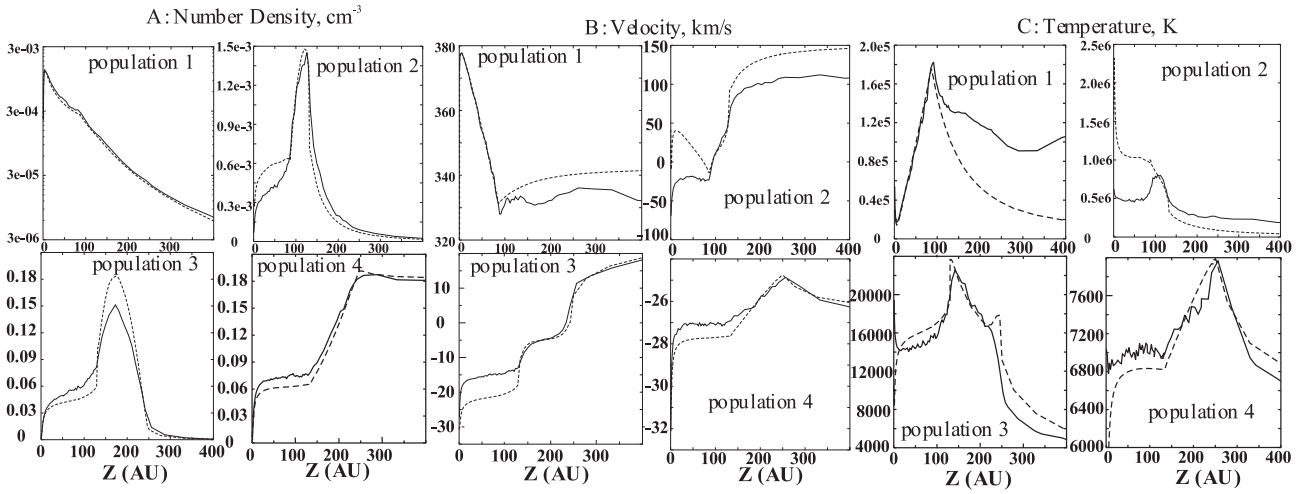

Fig. 5. The number densities (A), bulk velocitites (B), and temperatures (C) of the four populations of H atoms in the upwind direction for $K_{\rm fix}$ and $F4_{\rm fix}$ models. The solid and dashed curves correspond to $K_{\rm fix}$ and $F4_{\rm fix}$ models, respectively.

3.2. Role of McNutt's approximation of the source terms

To explore physical reasons for the differences identified above between self-consistent kinetic K and multi-fluid models, $F1-F4$, we need to examine two parts of the models: 1) the plasma part; and 2) the neutral part. Description of the plasma component is identical in all models with the only exception being the source terms in the right parts of the plasma Euler equations due to charge exchange. In the kinetic approach the source terms are calculated as corresponding integrals of velocity distribution function of H-atoms. In the multi-fluid models the integrals are taken under several assumptions (McNutt et al. 1998). One of the key assumptions made in order to get analytical expressions for the source terms is the assumption on Maxwellian (or sum of Maxwellians) behavior of the velocity distribution function of H atoms. Since the H-atom velocity distribution function is neither Maxwellian nor a sum of Maxwellians, some error is introduced at this stage.

To evaluate how large the error is we cannot use self-consistent models $F1$–$F4$, since the sources in these models are calculated based on different distributions of H-atoms. We performed five specific test cases, denoted as $K1$, $M1, M2, M3, M4$. In each of these cases we start with the same plasma distribution. Firstly, we run Monte-Carlo code to get both kinetically calculated source terms and a distribution of number density, bulk velocity, and kinetic temperature of H-atoms of the four introduced populations. Then to get the source terms of $M4$ model, we calculated the source terms $\boldsymbol{q}_2, q_3$ for each of the four populations according to McNutt et al. (1998). Number density, bulk velocity, and temperature of the H atoms calculated by Monte-Carlo are used in these calculations. Then we summarize the sources of individual populations and obtain the total source terms in the Euler plasma equations. In models $M2$–$M3$, we compute parameters of the interstellar population of H-atoms by summarizing number density of population 3 and 4 and calculating weighted averages for bulk velocity and temperature. In model $M2$, we do the same procedure of summarizing the population 1 and 2. In the model $M1$ we summarize all populations of H-atoms. Then we calculate source terms as described for $M4$ model. For each set of the source terms we solve plasma Euler equations numerically by our Godunov-type numerical code.

From the results of the numerical test calculations we conclude that the more fluids in the model, the smaller the difference with the kinetic model. Model $M4$ provides the closest results to the $K1$ model. The difference between $M4$ and $K1$ models is less than 1% in the distance to the termination and within 2.5% in the distances to the heliopause and the bow shock. Distributions of plasma parameters also demonstrate fairly good coincidence for $M4$ and $K1$ sets as compared with the plasma distributions in self-consistent $F4$ and K models. Therefore, $M4$ and $K1$ model results are closer to each other than are K and $F4$ model results.

One-fluid model $M1$ has the largest discrepancy with the kinetic model, up to 20% for the bow shock distance. Such a comparison naturally explains the cause of the difference between two available kinetic models, the Baranov-Malama and Müller-Zank-Lipatov models. Indeed, as described in Müller & Zank (2000), the source terms in the plasma equations are not calculated directly from the solution of the kinetic equation. Instead, the number density, bulk velocity, and kinetic temperature calculated by the particle mesh method were used in the analytical expressions of the source terms implying Maxwellian distribution of H atoms.

Finally, we conclude that approximation of the source terms in the Euler plasma equation by assuming Maxwellian distribution function produces significant differences in the location of the shocks and heliopause. The differences are especially large when all populations of H-atoms are treated as one-fluid. Nevertheless, in the cases, where the source terms in the Euler equations of the plasma component are calculated on the basis of the four-fluid H-atom approximation ($M4$ test case), the results are closer to the $K1$ model as compared with self-consistent K and $F4$ models. We conclude here that the main discrepancy between the four-fluid and kinetic approaches

cannot be explained by the approximation introduced by the analytical expressions of the source terms.

3.3. Comparison of H atom distribution in a fixed plasma field

Since we have shown that the four-fluid model gives the closest results to the kinetic model among other multi-fluid models, further in the paper we will only consider the four-fluid model. The goal of this subsection is to examine the four-fluid model for H-atoms compared to the kinetic model. Since the role of approximation of the source terms has already been explored and, in all other respects, the plasma codes are identical in both types of models, we fix the plasma distributions and consider H-atoms as test particles or test fluids that interact with the carrier plasma flow, but do not change it. In other words, we will compare results from the solution of kinetic and multi-fluid equations for H-atoms performed on the fixed plasma field, taken from the kinetic self-consistent solution (set K).

Figure 5 compares the densities, velocities, and temperatures of the four populations of H-atoms for the kinetic (solid curves) and four-fluid (dashed curves) models. In order to underline that these computations were performed for the fixed plasma field we denote these models as $K_{\rm fix}$ and $F4_{\rm fix}$ models. As previously for the self-consistent kinetic and 4-fluid models, the number densities, bulk velocities, and temperatures at the termination shock are different for $K_{\rm fix}$ and $F4_{\rm fix}$ models. The comparison indicates that multi-fluid models should be used to interpret data with great caution. It is seen that in the region, where a population of H atoms originates (e.g. inner heliosheath for population 2, outer heliosheath for population 3, supersonic solar wind for population 1) there is good coincidence between results of the $K_{\rm fix}$ and $F4_{\rm fix}$ models. The exception is the number density of population 3, which does not coincide in the entire computation region (Fig. 5A). Outside of the regions, where H atoms originate, parameters of H atoms are different almost everywhere. Interesting is that number densities and velocities of population 1 are rather close for $K_{\rm fix}$ and $F4_{\rm fix}$ models, while the behavior of temperature is different as discussed above. The flow of population 2 of H-atoms is subsonic in the supersonic solar wind region in the case of $F4_{\rm fix}$ model, and the Mach number is ~0.2 at 50 AU.

One can see from Fig. 5C that the kinetic temperature of H atom populations tends to be constant outside of the regions, where the populations originate. This behavior contrasts with behavior of the thermodynamic temperature of the $F4_{\rm fix}$ model. The difference is connected to the fact that the kinetic temperature is basically determined by energy sources and sinks due to charge exchange, while the thermodynamic temperature in $F4_{\rm fix}$ model is determined by the pressure, i.e. by effects connected with H-H collisions, which are artificially introduced into the fluid models.

3.4. Effect of charge exchange cross section

As observed in Fig. 5, the differences in number densities of population 3 of $K_{\rm fix}$ and $F4_{\rm fix}$ models in the outer heliosheath (where the atoms originated) are connected to production of the atoms, i.e. with destruction by charge exchange of H atoms of population 4. We performed numerical tests by varying the value of the cross section. The idea behind this set of numerical calculations was to obtain better agreement between kinetic and 4-fluid models by changing the mean free path of H atoms with respect to charge exchange. The test-calculations allow us to conclude that changing (in particularly, increasing) the cross section does not help to get better agreement between the kinetic and multi-fluid models. We explain this by the fact that in the multi-fluid models the mean free path of H atoms during collisions between those in one population is assumed to be much smaller than to both the characteristic size of the problem and the charge exchange mean free path of H atoms. Varying the charge exchange cross section by a factor of 2 does not change this relation between the two mean free paths. The effects of H-H collisions are dominant for all considered cases in the multi-fluid models, while the kinetic model corresponds to the realistic situation when the mean free path of H atoms with respect to H-H collision is larger than the characteristic size of the problem.

3.5. Effect of random thermal velocities

In order to explore the origin of the differences between the kinetic and four-fluid models let us focus on primary interstellar atoms (population 4) that serve as seed particles for all other populations, such that model differences for this population are translated to other populations of heliospheric H atoms. At the same time, consideration of this population is simpler, because distribution of this population depends only on the outer source of H atoms, which is the outer boundary, and on the distribution of the plasma component, which is chosen to be the same for the four-fluid and kinetic models.

As seen from above (e.g. Fig. 5), the number density, temperature, and velocity of this population are different in the four-fluid model as compared with the kinetic model. In particular, inside the heliopause the number density of H atoms in the kinetic model is larger than in the four-fluid model. Excluding the effect of the velocity dependence of the cross section, the only reason for this could be the atoms that can reach the upwind region at heliocentric distances smaller than 200 AU from the flanks. Such atoms exist in the kinetic model, while in the 4-fluid model particles should follow the streamlines, and the influence of the "side-effects" on the number density of H atoms in upwind appears indirectly through the pressure gradient term in the Euler equations and through change of the flux tubes.

Note that the possible reason for this difference in the number density of population 4 is, in fact, the direct consequence of the large mean free path of H atoms as assumed in the kinetic model and not assumed in 4-fluid model. In order to check this hypothesis we varied the temperature of the LIC and the temperature of the background plasma. Lower temperature corresponds to smaller thermal velocities of H atoms. Therefore, in the case of test calculations with artificially reduced temperature of the plasma component, we could expect better

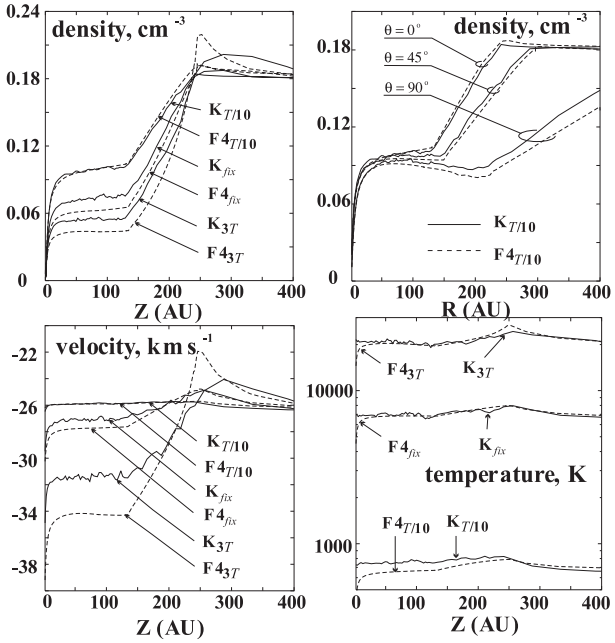

Fig. 6. The parameters of population 4 of H atoms for the models with the different temperature of background plasma field. The results given by kinetic (solid curves) and 4-fluid (dashed curves) models are presented to show the good agreement of the results for sets $K_{T/10}$ and $F4_{T/10}$.

agreement between the kinetic and four-fluid models. Figure 6 confirms this statement. We performed computations of the kinetic and four-fluid models for interstellar temperatures higher by a factor of 3 and lower by a factor of 10 than the "standard" interstellar temperature of ~6500 K. We denote these models as K_{3T}, $F4_{3T}$ and $K_{T/10}$, $F4_{T/10}$, respectively. Distributions of H atom number density, velocity, and temperature are shown in the figure. There is fairly good agreement between $K_{T/10}$ and $F4_{T/10}$ models, while the difference in the case of K_{3T} and $F4_{3T}$ models is larger than for $K_{\rm fix}$ and $F4_{\rm fix}$ models. Interestingly, the distributions of the H atom number densities of $K_{T/10}$ and $F4_{T/10}$ models coincide for the direction of 45 degrees from upwind, while in the sidewind direction (90 degrees of upwind) the difference becomes noticeable.

3.6. Effects of the outer source size

In the previous subsection we identified that the reason for the differences between kinetic and fluid models for population 4 is the differing transport of the H atom particles across the heliospheric interface. The effect of the thermal velocities was explored by varying the interstellar temperature. In this subsection we explore the same effect differently. Since we suggest that the main reason for the differences between the kinetic and fluid model results is in penetration of H atoms from the sides due to their large mean free path, we now change the source of H atoms in order to verify this effect. Up to now, the source of population 4 was the outer boundary of our computational domain. We performed several specific computations, where the flux of H atoms through the bow shock was restricted to those primary interstellar H atoms which have heliocentric angles $\theta < \theta_{\rm h}$ (see Fig. 1) at the bow shock. Outside the bow shock, computations were performed as previously. In other words, we assumed that the source area of H atoms penetrating inside the bow shock is a part of the bow shock surface restricted by the cone with angle $\theta_{\rm h}$ (Fig. 1). We performed numerical calculations of both the kinetic and four-fluid models for different $\theta_{\rm h}$ angles: $\theta_{\rm h} = 4.5°$, 13.5°, 22.5°, 45°. These models we denote as $K_{\theta_{\rm h}=4.5°}$, $F_{\theta_{\rm h}=4.5°}$, $K_{\theta_{\rm h}=13.5°}$, $F_{\theta_{\rm h}=13.5°}$, $K_{\theta_{\rm h}=22.5°}$, $F_{\theta_{\rm h}=22.5°}$, $K_{\theta_{\rm h}=45°}$, respectively. In addition, we performed similar calculations with reduced and increased interstellar temperature: $K_{\theta_{\rm h}=4.5°;T/10}$, $K_{\theta_{\rm h}=4.5°;3T}$, $K_{\theta_{\rm h}=9°;T/10}$, $K_{\theta_{\rm h}=13.5°;3T}$, $K_{\theta_{\rm h}=45°;3T}$ models. We did the simulations for different temperatures in order to get an idea of the number of particles coming from the sides (Fig. 7). In the case of low temperature (models $K_{T/10}$, $K_{\theta_{\rm h}=4.5°;T/10}$, $K_{\theta_{\rm h}=9°;T/10}$), the angle of $\theta_{\rm h} = 9°$ is enough to practically reproduce $K_{T/10}$-model results. In the case of high temperature (models $K_{\theta_{\rm h}=4.5°;3T}$, $K_{\theta_{\rm h}=13.5°;3T}$, $K_{\theta_{\rm h}=45°;3T}$), this angle is 45°, while in the case of the realistic interstellar temperature the angle is somewhere in between, ~25°. It is interesting to note that inside 250 AU, the number density of H atoms is larger in the case of low temperature models than in the large temperature models. This is connected to the fact that in the case of low temperature the velocities of individual atoms weakly deviate from the bulk velocity of the interstellar gas, while in the case of hotter plasma there are more particles which escape from upwind due to their large thermal velocities.

Comparison of the kinetic and fluid models for different sizes of the outer source of H atoms is shown in Fig. 7A. It is seen that there is a good agreement between results of the models with low values of $\theta_{\rm h}$: $\theta_{\rm h} = 4.5°$ and $\theta_{\rm h} = 13.5°$. For larger $\theta_{\rm h}$, e.g. $\theta_{\rm h} = 22.5°$ (models $K_{\theta_{\rm h}=22.5°}$, $F_{\theta_{\rm h}=22.5°}$), the results of the kinetic and four-fluid models are different. This is the direct demonstration of the kinetic behavior of the H atom flow and of the effects of the mean free path that is comparable to the size of the interface.

Results of numerical test presented in Fig. 7 clearly demonstrate that so-called "zones of dependence" of the solution are different in the kinetic and multi-fluid models. Number densities of $F_{\theta_{\rm h}=22.5°}$ and $F_{\rm fix}$ models practically coincide, while for $K_{\theta_{\rm h}=22.5°}$ and $K_{\rm fix}$ they are still different. This difference in "zones of dependence" between the kinetic and multi-fluid models is a reflection of fundamental differences between the kinetic and multi-fluid approaches.

4. Conclusions

In this paper we compare results of the different self-consistent heliospheric interface models with kinetic and multi-fluid descriptions of the interstellar H atoms. In addition to existing kinetic Baranov-Malama model, we developed four different multi-fluid models for the interstellar H atoms and performed a number of test calculations. We conclude that:

1. Flow of the interstellar H atoms in the heliospheric interface must be described kinetically. The multi-fluid approach as applied to the interstellar H atoms leads to different results than the kinetic approach. It was shown that the differences in number density, velocity, and temperature of the

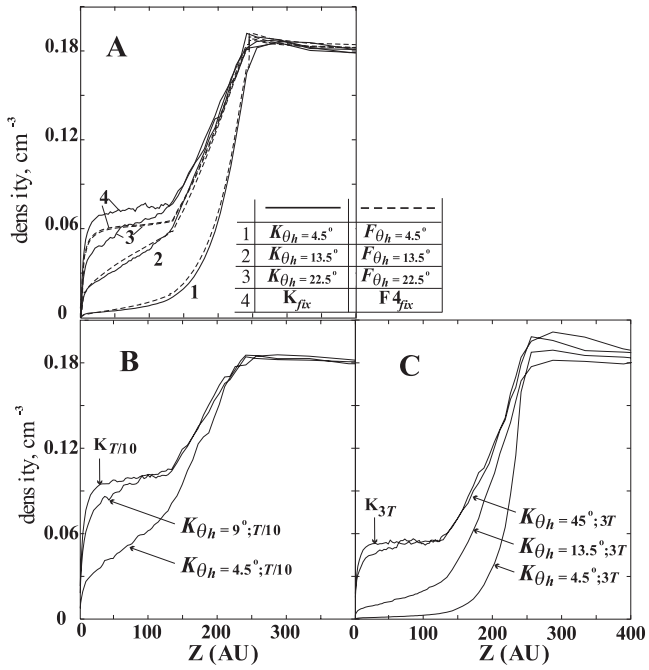

Fig. 7. The number density of population 4 in the upwind direction. Solid and dashed curves in Fig. 7A correspond to kinetic and 4-fluid models, respectively.

interstellar H atoms inside the heliosphere and at the termination shock obtained in the kinetic and multi-fluid models are significant. Therefore, using the multi-fluid models will affect how observational data are interpreted, including pickup ion spectra measured onboard Ulysses and ACE and backscattered solar Lyman-alpha radiation measured by SOHO/SWAN, HST, Voyager 1 and 2, Pioneer 10, etc. The same conclusion can be made for the fluxes of the atoms originating in the inner heliosheath, which are known as the heliospheric ENAs and will be measured by Interstellar Boundary Explorer (`http://www.ibex.swri.edu`) in the very near future.

2. The fundamental difference between the kinetic and multi-fluid approaches for the H atom component in the heliospheric interface is that the multi-fluid models are based on voluntary assumption that the flow of H atoms can be described hydrodynamically by a set of Euler equations (one-fluid approach) or by 2, 3, and 4 sets of Euler equations for different populations of the H atoms (2-, 3-, or 4- fluid models, respectively). Physically, this assumption means that the mean free path of H-H collisions between the H atoms of one population is effectively smaller than both the characteristic size of the problem and the mean free path with respect of charge exchange. At the same time, H-H collisions between H atoms of different populations are ignored in the multi-fluid approaches.

3. By a number of numerical tests for different cross-sections, different temperatures of the background plasma, and different outer sources of the interstellar particles, we established that the fundamental reason for the difference in the results of the kinetic and four-fluid models for the primary interstellar H atom component lies in different "zone of influences" of the solution in the kinetic and fluid approximations. In other words, the reason for the difference is in the amount of particles that come from the side of the streamlines of the H atom flow and contribute to the velocity distribution of H atoms. In the kinetic model particles from the sides are contribute easily to the H-atom population at a certain point due to their large mean free paths. In the fluid approaches, the flow outside of a flux-tube could indirectly contribute through the change in the streamlines and, therefore, in the tube size. The behavior of flow in the fluid-models is determined by artificially introduced H-H collisions among the atoms inside of one-population.

4. The results obtained with the four-fluid model, which describes interstellar H-atoms as a sum of four Maxwellian populations, are the closest to results of kinetic description compared to other multi-fluid models. By comparing the kinetic and four-fluid models we established that approximation of the source terms in the plasma Euler's equations by McNutt et al. (1998), which assumes that the velocity distribution function of H atoms is the sum of four shifted Maxwellians, is not the main source of discrepancies between kinetic and multi-fluid models. At the same time the use of this approximation for the source terms in one-, two-, three- fluid models results in large differences with the kinetic model.

5. Finally, from the consideration above and fundamental differences between kinetic and fluid approximations, we conclude that we cannot find any way to improve the multi-fluid models of H atoms in order for their results to approach those of the kinetic model. Instead, the kinetic approach should be used for future 3D modelling of H atoms in the heliospheric interface.

Significant new constraints on the heliospheric interface models will be obtained in the nearest future from the analysis of backscattered Lyman-alpha data collected over nearly the whole solar cycle by SOHO/SWAN (see, e.g., Lallement et al. 2005) and from the future NASA Interstellar Boundary Explorer (IBEX; `http://ibex.swri.edu`) mission, which is planned for launch in 2008 (see, McComas et al. 2004). Other important constraints will be obtained from analysis of Ulysses/SWICS pickup ion data, of Voyager 1/2 plasma and magnetic field data, and of other diagnostics. Comparison of model predictions with data will determine whether the models described above and their future progress will be able to explain the observational data adequately. However, it is important that the models used for the interpretation should have a solid theoretical background.

Acknowledgements. We thank Yu. Malama for numerous helpful discussions and for his Monte-Carlo code, and A. Myasnikov for his gasdynamic code. The calculations were performed on the supercomputer of the Russian Academy of Sciences. This work was supported in part by INTAS Award 2001-0270, RFBR grants 04-02-16559, 04-01-00594, RFBR-GFEN grant 03-01-39004, Program of Basic Researches of OEMMPU RAS, NASA grant NNG05GD69G, and the International Space Science Institute in Bern.

References

Alexashov, D. B., Baranov, V. B., Barsky, E. V., & Myasnikov, A. V. 2000, Astron. Let., 26, 743

Alexashov, D. B., Izmodenov, V. V., & Grzedzielski, S. 2004a, Adv. Space Res., 34, 109

Alexashov, D. B., Chalov, S. V., Myasnikov, A. V., Izmodenov, V. V., & Kallenbach, R. 2004b, A&A, 420, 729
Baranov, V. B., Lebedev, M. G., & Malama, Yu. G. 1991, ApJ, 375, 347
Baranov, V. B., & Malama, Yu. G. 1993, J. Geophys. Res., 98, 15157
Baranov, V. B., & Malama, Yu. G. 1995, J. Geophys. Res., 100, 14755
Baranov, V. B., & Malama, Yu. G. 1996, Space Sci. Rev., 78, 305
Baranov, V. B., Izmodenov, V., & Malama, Yu. G. 1998, J. Geophys. Res., 103, 9575
Florinski, V., Pogorelov, N., & Zank, G. 2003, J. Geophys. Res. 108(A6), 1228
Florinski, V., Pogorelov, N., Zank, G., Wood, B., & Cox 2004, ApJ, 604, 700
Fahr, H. J. 2000, Ap&SS, 274, 35
Fahr, H. J., Kausch, T., & Scherer, H. 2000, A&A, 357, 268
Gloeckler, G., & Geiss, J. 2004, Adv. Space. Res., 34, 53
Gloeckler, G., Möbius, E., Geiss, J., et al. 2004, A&A, 426, 845
Godunov, S. K. (Ed.) 1979, Résolution numérique des problèmes multidimensionnels de la dynamique des gaz (Moscow: Editions MIR)
Gruntman, M., Roelof, E., Mitchell, D., et al. 2001, J. Geophys. Res., 106, 15767
Hirsch, C. 1990, Numerical Computation of internal and external flows (John Willey and Sons), 691
Izmodenov, V. V. 2000, Ap&SS, 274, 55
Izmodenov, V. V. 2001, Space Sci. Rev., 97, 385
Izmodenov, V. V. 2003, Proc. of the Interstellar enviroment of the heliosphere, COSPAR Colloquium in Honour of Stanislaw Grzedzielski, ed. D. Breitschwerdt, & G. Haerendel, MPE Report, 285, 113
Izmodenov, V. V. 2004, Chapter 2 in The Sun and the Heliosphere as an Integrated System Series: Astrophysics and Space Science Library, 317, ed. G. Poletto, & S. T. Suess
Izmodenov, V. V., & Alexashov, D. 2003, Astron. Let., 29, 58
Izmodenov, V., & Malama, Yu. G. 2004a, AIP Conf. Proc., 719, 47
Izmodenov, V., & Malama, Yu. G. 2004b, Adv. Space Res., 34, 74
Izmodenov, V. V., Geiss, J., Lallement, R., et al. 1999, J. Geophys. Res., 104, 4731
Izmodenov, V. V., Malama, Y. G., Kalinin, A. P., et al. 2000, Ap&SS, 274, 71
Izmodenov, V., Gruntman, M., & Malama, Yu. G. 2001a, J. Geophys. Res., 106, 10681
Izmodenov, V., Gruntman, M., Baranov, V., & Fahr, H. 2001b, Space Sci. Rev., 97, 413
Izmodenov, V., Gloeckler, G., & Malama, Yu. G. 2003a, Geophys. Res. Let., 30, 1351
Izmodenov, V. V., Malama, Yu. G., Gloeckler, G., & Geiss, J. 2003b, ApJ, 594, L59
Izmodenov, V., Malama, Yu. G., Gloeckler, G., & Geiss, J. 2004, A&A, 414, L29
Izmodenov, V., Malama, Yu. G., & Ruderman, M. S. 2005, A&A, 429, 1069
Karmesin, S. R., Liewer, P. C., & Brackbill, J. U. 1995, Geophys. Res. Let., 22, 1153
Krimigis, S. M., Decker, R. B., Hill, M. E., et al. 2003, Nature, 426, 45
Lallement, R., Raymond, J. C., Vallerga, J., et al. 2004a, A&A, 426, 875
Lallement, R., Raymond, J. C., Bertaux, J.-L., et al. 2004b, A&A, 426, 867
Lallement, R., Qumerais, E., Bertaux, J.-L., et al. 2005, Science, 307, 1447
Lipatov, A. S., Zank, G. P., & Pauls, H. L. 1998, J. Geophys. Res., 103, 20631
Maher, L. J., & Tinsley, B. A. 1977, J. Geophys. Res., 82, 689
Malama, Yu. G. 1991, Ap&SS, 176, 21
Malama, Yu. G., Izmodenov, V. V., & Chalov, S. V. 2005, JGR, submitted
McComas, D., Allegrini, F., Bochsler, P., et al. 2004, AIP Conf. Proc., 719, 162
McDonald, F. B., Stone, E. C., Cummings, A. C., et al. 2003, Nature, 426, 48
McNutt, R. L. Jr., Lyon, J., & Goodrich, C. C. 1998, J. Geophys. Res., 103, 1905
McNutt, R. L., Lyon, J., & Goodrich, C. C. 1999, J. Geophys. Res., 104, 14803
McNutt, R. L., Jr., Wiltberger, M., Lyon, J., & Goodrich, C. C. 2001, COSPAR Coll. Ser., 11, 89
McNutt, R. L. 2003, AIP Conf. Proc., 679, 194
McNutt, R. L. 2004, AIP Conf. Proc., 719, 111
Müller, H.-R., Zank, G. P., & Lipatov, A. S. 2000, J. Geophys. Res., 105, 27419
Möbius, E., Bzowski, M., Chalov, S., et al. 2004, A&A, 426, 897
Myasnikov, A., Alexashov, D., Izmodenov, V., & Chalov, S. 2000, J. Geophys. Res., 105, 5167
Myasnikov, A. V., Belov, N. A., & Zhekov, S. A. 1997, Preprint 582 of Institute for Problems in Mechanics RAS
Osterbart, R., & Fahr, H.-J. 1992, A&A, 264, 260
Pauls, H. L., & Zank, G. P. 1997, J. Geophys. Res., 102, 19779
Richardson, J. D. 1997, Geophys. Res. Let., 24, 2889
Richardson, J. D., Wang, C., & Burlaga, L. F. 2004, Adv. Space Res., 34, 150
Scherer, K., & Fahr, H. J. 2003a, Geophys. Res. Let., 30
Scherer, K., & Fahr, H. J. 2003b, Ann. Geophys., 21
Wang, C., & Belcher, J. W. 1998, J. Geophys. Res., 103, 247
Wang, C., & Belcher, J. W. 1999, J. Geophys. Res., 104, 549
Wang, C., & Richardson, J. D. 2003, J. Geophys. Res. 108, SSH 1-1
Witte, M. 2004, A&A, 426, 835
Zank, G., & Müller, H. 2003, J. Geophys. Res., 108, A6, pp. SSH 7-1, CiteID 1240
Zank, G. P., Pauls, H. L., & Williams, L. L. 1996, J. Geophys. Res., 101, 21639